Nonequilibrium reservoir engineering of a biased coherent conductor for hybrid energy transport in nanojunctions

Bing-Zhong Hu, Tao Wang, Lei-Lei Nian,* and Jing-Tao Lü†
School of Physics and Wuhan National High Magnetic Field Center, Huazhong University of Science and Technology, Wuhan 430074, P. R. China

(Dated: January 14, 2019)

We show that a current-carrying coherent electron conductor can be treated as effective bosonic energy reservoir involving different types of electron-hole pair excitation. Hybrid energy transport between nonequilibrium electrons and bosons can be described by a Landauer-Büttiker formula. This allows for simple, unified account of a variety of heat transport problems in hybrid electron-boson systems, including non-reciprocal heat transport, thermoelectric current from a cold-spot and radiative cooling. Our general framework opens the way of nonequilibrium reservoir engineering for efficient energy control in the nanoscale.

I. INTRODUCTION

Understanding nonequilibrium energy transport in the nanoscale is of crucial importance both for the fundamental development of quantum thermodynamics and for the practical application of nanoscale thermoelectric and optoelectronic devices. For phase coherent transport, the celebrated Landauer-Büttiker formalism has been successfully applied to study quasi-particle energy transport following different statistics, including electrons[1], photons[2–5], phonons[6–15] and magnons[16]. Wherein, the baths connecting to the system are assumed to be in thermal equilibrium with given temperature and/or chemical potential, with the quasi-particle distribution function determined by its statistics, i.e., the Fermi-Dirac distribution for fermions, and the Bose-Einstein distribution for bosons. A difference in the distribution drives an energy current flow between the two thermal baths.

However, the same approach is difficult to describe energy transport between quasi-particles following different statistics, which is ubiquitous in thermoelectric and optoelectronic processes of nano-junctions. Examples of such processes include electroluminescence[17–20], Joule heating[21–26], current-induced[24, 27–29] or radiative cooling[30]. Another difficulty arising in these processes is that the quasi-particles may be in nonequilibrium state due to driving from external bias.

In this work, we overcome this difficulty by 'bosonizing' a voltage-biased coherent electron conductor into a bosonic reservoir with non-zero chemical potential. We obtain a Landauer formula to describe energy transport between electrons and bosons. This is possible since energy transport between electrons and bosons is always accompanied by the generation or annhilation of different kinds of electron-hole pairs (EHPs)[31, 32]. We thus generalizes the Landauer-Büttiker formalism to hybrid energy transport between possibly nonequilibrium baths, and provides a unified framework to understand energy transport in different thermal, thermoelectric and optoelectronic processes.

II. THEORY

A. System setup

Model.– We consider a model system schematically shown in Fig. 1 (a). The *system* composed of an independent set of bosonic degrees of freedom (DOF) taken as a set of harmonic oscillators. It couples to two kinds of baths. One is an equilibrium boson bath (ph-bath), modeled by an infinite number of harmonic oscillators. The other is an electron bath (e-bath), which itself includes a central part (C) and two electrodes (L and R). The e-bath may be driven into a nonequilibrium steady state by a voltage bias applied between the two electrodes. Without loss of generality, we assume that the system couples only to the central region of the e-bath. Energy transport between the two baths takes place through their simultaneous coupling to the system. The electrons couple to the 'displacement' of the system harmonic oscillators

$$H_{es} = \sum_{i,j,k} M_{ij}^k c_i^\dagger c_j u_k. \tag{1}$$

Here, M_{ij}^k describes the coupling of the system mode k to the electronic transition between states i and j, and u_k is the 'displacement' operator of the system mode k. For phonons, it is the displacement, while for photons it is the vector potential. The system-ph-bath coupling is linear between harmonic oscillators and can be treated exactly.

B. Electron-hole pair excitation

Our key observation is that the energy transport between the system and the electron bath can be modeled by different kinds of reactions between EHPs in the e-bath and the bosonic modes in the system. The creation

* llnian@hust.edu.cn
† jtlu@hust.edu.cn

and annihilation of the bosonic mode is always accompanied by the recombination and creation of EHPs. These processes can be expressed in the form of reactions

$$e_\alpha + h_\beta \rightleftharpoons b_n, \tag{2}$$

where e_α, h_β and b_n represent electron in electrode α, hole in electrode β and bosonic mode b_n in the system. Equivalently, we can write

$$e_\alpha \rightleftharpoons e_\beta + b_n, \tag{3}$$

representing inelastic electronic transition from electrode α to β, accompanied by emission of bosonic mode n (forward process). The backward direction corresponds to absorption process.

There are four types of EHPs which we label by the spatial location of the electron (α) and hole (β) states. They are schematically shown in Fig. 1 (c) and (d) for recombination and creation processes, respectively. They are denoted by EHP-i ($i = 1, 2, 3, 4$) and are further divided into two groups. The intra-electrode type includes $1/LL$ and $2/RR$, and inter-electrode type includes $3/RL$, $4/LR$. Additional to energy transfer between e-bath and system, the generation and recombination of inter-electrode EHPs also involves charge transport across the system. We take the energy of mode and the EHPs to be positive.

A generalized detailed balance relation applies to each of reactions

$$\frac{T_{\alpha\rightharpoonup\beta}}{T_{\alpha\leftharpoondown\beta}} = \exp\left[-\beta_B(\hbar\Omega - \mu_{\alpha\beta})\right]. \tag{4}$$

Here, $T_{\alpha\rightharpoonup\beta}$ and $T_{\alpha\leftharpoondown\beta}$ are the reaction rates for the forward (boson emission) and backward (boson absorption) processes in Eq. (2), respectively. They are obtained from the Fermi golden rule

$$T_{\alpha\rightharpoonup\beta} = \frac{2\pi}{\hbar}\sum_{i\in\alpha, f\in\beta} |M_{ij}^m|^2 \delta(\varepsilon_i - \varepsilon_f - \hbar\Omega) \times n_F(\varepsilon_i - \mu_\alpha)(1 - n_F(\varepsilon_f - \mu_\beta)). \tag{5}$$

Here, $n_{F/B}(\varepsilon, T) = [\exp(\beta_B\varepsilon) \pm 1]^{-1}$ is the Fermi-Dirac/ Bose-Einstein distribution, with $\beta_B = (k_B T)^{-1}$, $\mu_{\alpha\beta} = \mu_\alpha - \mu_\beta$, and $M_{ij}^m = \langle\psi_i(\varepsilon_i)|M|\psi_f(\varepsilon_f)\rangle$ is the transition matrix element from initial state i in electrode α to final state f in electrode β. The reverse rate $T_{\alpha\leftharpoondown\beta}$ can be written similarly. Thus, when reaching equilibrium with the EHP bath $\alpha\beta$, the bosonic mode follows a Bose-Einstein distribution at temperature T_e and chemical potential $\mu_{\alpha\beta}$. For intra-electrode processes, $\mu_{\alpha\beta} = 0$, we have the normal detailed balance relation, while for inter-electrode processes $\mu_{\alpha\beta}$ is determined by the applied voltage bias. Thus, the boson mode may acquire a non-zero chemical potential in nonequilibrium. This is consistent with the equilibrium condition for reaction 2.

The key quantity to describe the EHP baths is the coupling-weighted power spectrum. It can be written as

$$\tilde{\Pi}_{mn}^{\alpha\beta}(\omega) = \left[n_B(\hbar\omega - \mu_{\alpha\beta}, T_e) + \frac{1}{2}\right]\Lambda_{mn}^{\alpha\beta}(\omega). \tag{6}$$

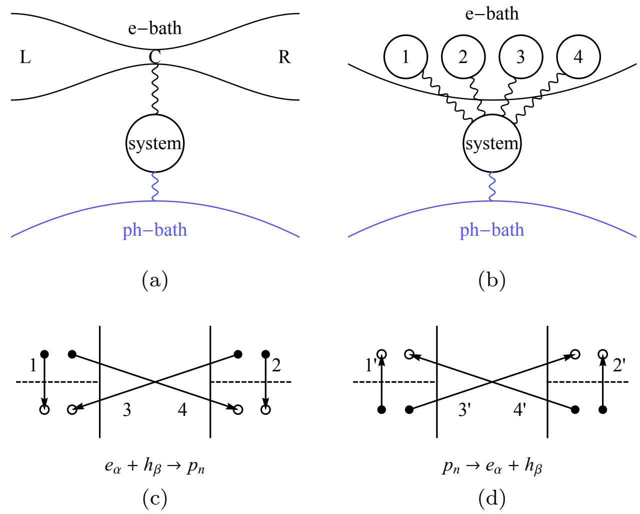

FIG. 1. (a) Schematics of the model we consider. The system consists a set of independent bosonic modes. It couples to an electron bath (e-bath), which is modeled as a conductor including a left (L) and a right (R) electrode, with temperature T_e and chemical potential μ_L and μ_R, respectively. The system further couples to an external thermal bath (ph-bath) at temperature T_{ph}. (b) The electron bath can be treated as four different kinds of electron-hole pair (EHP) baths (1-4), shown in (c). (c-d) Four kinds of EHP recombination (c) and excitation (d) processes. The EHPs are classified according to the spatial location of the electron (e_α) and the hole (h_β). (1,1') Both are at electrode L, (2,2') Both are at electrode R, (3,3') The electron at electrode R and a hole at electrode L. (4,4') The electron at electrode L and a hole at electrode R. removing (d)?

We have introduced the coupling-weighted EHP density of states (DOS)[33, 34]

$$\begin{aligned}\Lambda_{mn}^{\alpha\beta}(\omega) &= -\sum_{i\in\alpha, f\in\beta} M_{fi}^m M_{if}^n \delta(\varepsilon_i - \varepsilon_f - \hbar\omega) \\ &\quad\times (n_F(\varepsilon_\alpha - \mu_\alpha, T_\alpha) - n_F(\varepsilon_\beta - \mu_\beta, T_\beta)) \\ &= -\int \frac{d\varepsilon}{2\pi}\mathrm{tr}[M^m A_\alpha(\varepsilon) M^n A_\beta(\varepsilon - \hbar\omega)] \\ &\quad\times (n_F(\varepsilon - \mu_\alpha, T_\alpha) - n_F(\varepsilon - \hbar\omega - \mu_\beta, T_\beta)),\end{aligned} \tag{7}$$

which also characterizes the system dissipation due to coupling to the e-bath[33]. Equation (6) follows a form of the fluctuation-dissipation relation for an equilibrium boson bath, albeit with a possibly non-zero chemical potential $\mu_{\alpha\beta}$. The intra-electrode EHPs (i=1,2) are always in equilibrium with $\mu_{\alpha\alpha} = 0$ and temperature T_e. But the two inter-electrode EHPs (i=3, 4) have opposite chemical potential $\mu_{RL} = -\mu_{LR}$. They are non-zero when there is a voltage bias applied. To this end, we have shown that the *nonequilibrium* e-bath can be divided into four *equilibrium* EHP baths with different chemical potentials. This effective model is shown in Fig. 1 (b).

C. Energy transport

Within this effective EHP model, hybrid energy transport between electrons and system bosons can be treated as bosonic transport. To the lowest order approximation, we arrive at a Landauer-Büttiker formula for the energy transport from e-bath to the system as a summation of contributions from all the EHP baths

$$J = \sum_{\alpha,\beta} \int_0^{+\infty} \frac{d\omega}{2\pi} \hbar\omega \ \mathrm{Tr}[\Lambda^{\alpha\beta}(\omega) \mathcal{A}_{ph}(\omega)] \times [n_B(\omega - \mu_{\alpha\beta}, T_e) - n_B(\omega, T_{ph})]. \quad (8)$$

Here, T_e and T_{ph} are the temperature of the e-bath and ph-bath, respectively. The trace Tr is over system DOF, with $\mathcal{A}_{ph} = D^r \Gamma_{ph} D^a$ the spectral function of the system due to coupling to the ph-bath. The summation over $\alpha\beta$ includes contributions from all the four types of EHPs. Each of them contributes to an energy transport channel.

In the following we show several applications of this central result. To be more specific, we consider a minimum model of the e-bath shown in Fig. 2. We have two electronic states 1 and 2 (on-site energies ε_1 and ε_2) couple to the electrodes L and R with coupling parameter γ_1 and γ_2, respectively. Electron hopping between the two states is assisted by one bosonic mode, which at the same time couples to a ph-bath with coupling constant γ_{ph}.

III. APPLICATIONS

A. Non-reciprocal heat transport

Firstly, we consider the situation where the e-bath and ph-bath are in their own thermal equilibrium at two different temperature T_e and T_{ph}. This indicates that $\mu_L = \mu_R$ and $T_L = T_R = T_e$. If we ignore the energy dependence of A in Eq. (7), $\Lambda_{mn}(\omega) = \hbar\omega \mathrm{tr}[M^m A M^n A]$ with $A = A_L + A_R$. Consequently, the transmission $\mathcal{T} = \mathrm{Tr}[\Lambda \mathcal{A}_{ph}]$ does not depend on T_e. Equation (8) reduces to the Landauer formula for heat transport between two harmonic thermal baths. Thus, the EHPs behave as linear harmonic oscillator thermal baths.

On the other hand, if we consider the energy dependence of $A(\varepsilon)$, $\Gamma(\omega)$, $\mathcal{T}$ will depend on T_e. Energy transport becomes nonlinear. In this case, non-reciprocal energy flow is possible, i.e., $J(\Delta T) \neq J(-\Delta T)$, with $\Delta T = T_e - T_{ph}$. We thus find a necessary condition for non-reciprocal energy transport in a hybrid electron-boson system: the electron DOS in the thermal window near the chemical potential has to be energy dependent[35, 36]. For normal metal electrode, the energy scale of electrons is much larger than the thermal energy, leading to a flat DOS. The energy dependence of $A(\varepsilon)$ can be engineered by changing the electronic states of the central part. For example, discrete energy levels of a molecular junction or quantum dot can be used.

In Fig. 3 we have considered a two-dot junction shown in Fig. 2. We set $\mu_L = \mu_R$ and $T_e \neq T_{ph}$ to consider heat transport. The electronic DOS shows an energy dependent Lorentzian shape. This gives rise to non-reciprocal heat transport between e-bath and ph-bath.

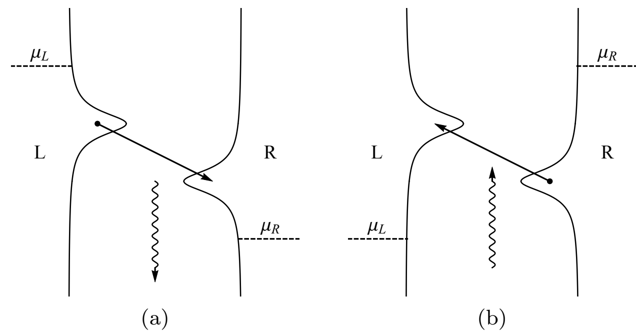

FIG. 2. Two limiting cases of nonequilibrium reservoir engineering. In (a), we have a filled electronic level ε_L that couples to the left electrode with chemical potential μ_L, and an empty level ε_R that couples to the right electrode with chemical potential μ_R. We have $\mu_L > \mu_R$. Heating of the bosonic mode is due to resonant recombination of inter-electrode (process 4 in Fig. 1). In (b), the situation is reversed. The left state ε_L is empty, while the right state ε_R is filled. When $\mu_R > \mu_L$, the e-bath can be used to cool the bosonic mode through creation of inter-electrode EHPs (process 4' in 1).

B. Hybrid thermoelectric transport

We can also study the thermoelectric transport of the temperature-biased electron-boson junction. When $T_{ph} \neq T_e$, in addition to the heat transport between system and e-bath, an electrical current may also be induced between the two electrodes[37, 38]. In our EHP picture, this is realized through coupling of the bosonic mode with two inter-electrode EHPs. Since they contribute to two electrical current with opposite directions, in order to get a non-zero electrical current, these two channels should not get canceled. The resonant situation in Fig. 2 can be used to enhance one of the two channels. In Fig. 4, we show the thermoelectric current induced by the temperature different ΔT for different chemical potentials $\mu_L = \mu_R$. The current is the largest when the chemical potential is in between ε_L and ε_R, where the resonant enhancement is the most prominent.

Previously, electrical current generated from a phonon hot-spot ($T_{ph} > T_e$) has been considered[37]. Our results show that the opposite is also possible, where electricity is generated by cooling the ph-bath. This demonstrates the decoupling of heat and charge transport as an advantage of thermoelectricity in hybrid nano-junctions.

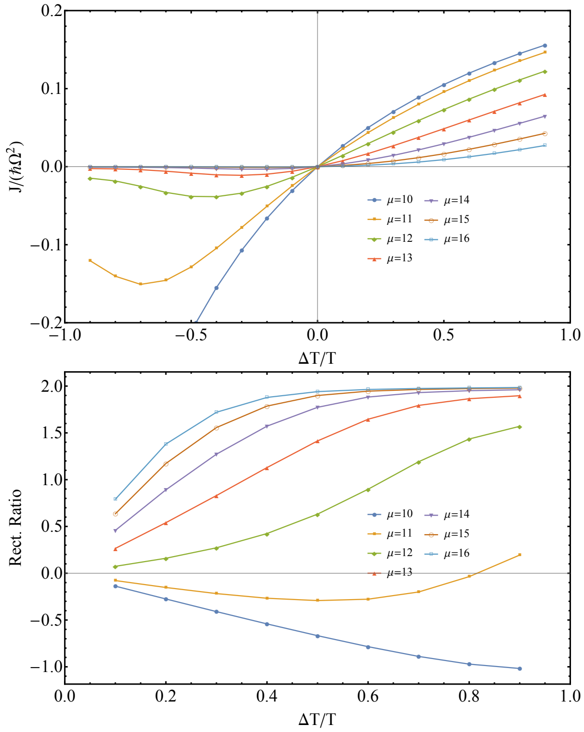

FIG. 3. Non-reciprocal heat transport in a double dot junction shown in Fig. 2 (a). (a) Heat current as a function of temperature difference ΔT for different chemical potentials. (b) Rectification ratio as a function of ΔT for different chemical potentials. We consider only one bosonic mode, whose energy is taken as unit energy. The following parameters are used: $\varepsilon_L = 10.5$, $\varepsilon_R = 9.5$, $\mu_L = \mu_R$, $\gamma_L = \gamma_R = 0.5 = m = 0.5$, $\hbar\Omega = 1$, $k_B = 1$.

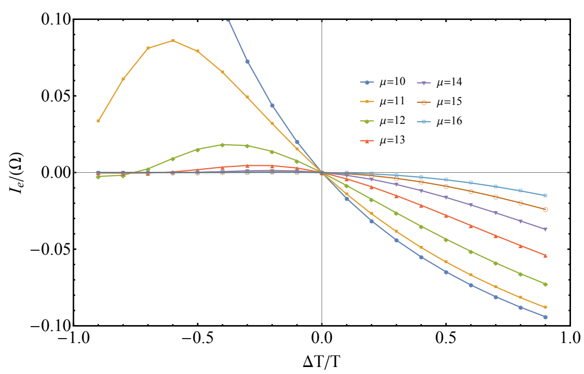

FIG. 4. Thermoelectric current generation from temperature difference between e-bath and ph-bath ΔT. The paremeters are the same as Fig. 3.

C. Electronic cooling of bosonic mode

We now turn on the voltage bias in the e-bath. The applied voltage changes the initial and final electron states of the EHP excitation. Thus, the EHP DOS can be modified by voltage. More importantly, the inter-electrode EHPs acquire a non-zero chemical potential, given by $\pm\mu_{RL}$ respectively. We assume $eV = \mu_L - \mu_R > 0$ without loss of generality. The EHP-4 has a chemical potential of $-eV$, while EHP-3 gets a chemical potential with opposite value eV. Change of the chemical potential breaks the equilibrium in the reaction, and drives the energy transport between e-bath and the system. Direction of energy flow depends on the relative magnitude of two fluxes. It can be engineered by tuning the electronic band structure, or more specifically, the transition probability of the two types of EHP excitation.

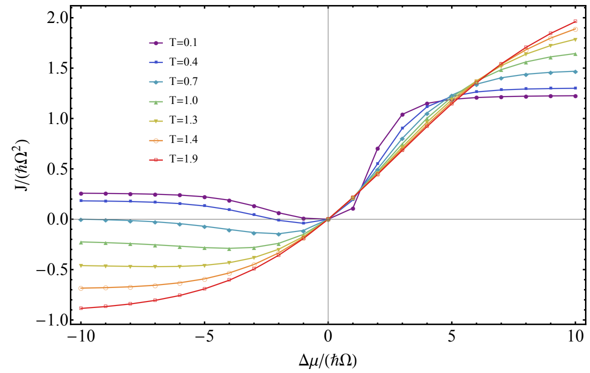

FIG. 5. Energy current from the e-bath to the bosonic mode as a function of applied bias, corresponding to the situation in Fig. 2 (b). Negative J means cooling of the bosonic mode.

Figure 2 shows two limiting cases. In Fig. 2 (a), process 4 is enhanced due to resonant inelastic electron tunneling when the separation between the two DOS peaks is resonant with energy of the bosonic mode. Consequently, energy flows from e-bath to the system. In Fig. 2 (b), process 4' is resonantly enhanced, resulting in energy flow in the opposite direction. Electronic cooling becomes possible using this resonant enhancement. This is demonstrated in Fig. 5, where the heat current from the e-bath to the system is plotted as a function of voltage bias $\mu_L - \mu_R$ while keeping temperature fixed $T_e = T_{ph} = T$. For negative bias, we observe a negative J regime. The range of this regime gets larger for higher temperature T. This is the electronic cooling of the bosonic mode. Very recently, experimental demonstration of near field radiative cooling using a reversely biased p-n junction has been demonstrated [30]. The experimental results can be understood using this simple model.

D. Current-induced exceptional point in two-mode system

So far, we have only considered one bosonic mode in the system. Now we show that the nonequilibrium e-bath can be used to couple two otherwise isolated bosonic modes. The bias dependence of coupling parameters can be used to tune the system to an exceptional point, where both the eigen values and eigen vectors of the two modes coalesce.

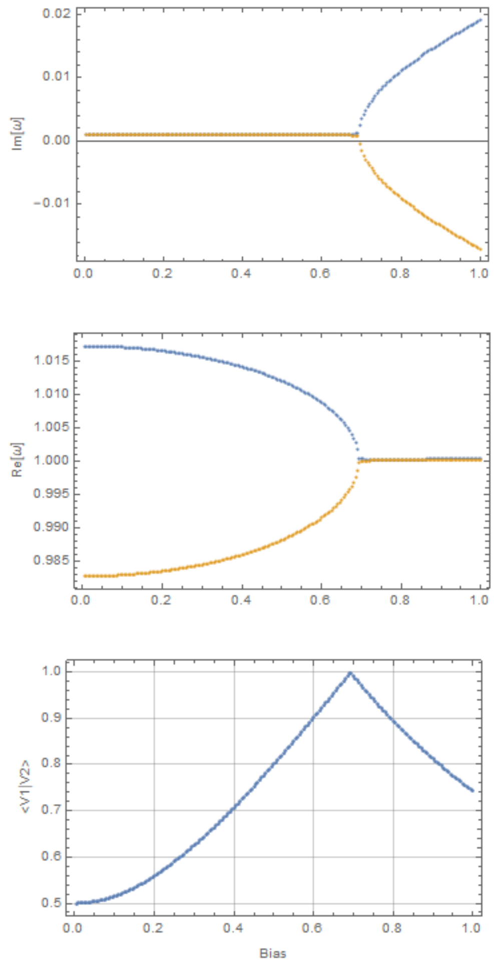

FIG. 6. Emergence of exceptional point due to coupling to a nonequilibrium e-bath. The effective dynamical matrix is given in Eq. (9). The following parameters are used: $\Omega = 1$, $\delta = 0.04$, $\gamma = 0.001$, $a = 0.05$, $b = 0.0$, $c = 0.02$.

To illustrate this effect, we consider two identical bosonic modes with average frequency Ω and a small detuning δ, such that $\omega_\pm = \Omega \pm \delta/2$. Extra damping of the two modes γ_1 and γ_2 are introduced to account for their coupling to e-bath and ph-bath. Importantly, the nonequilibrium nature of the e-bath introduces coherent coupling between the two otherwise isolated modes, which are proportional to the applied bias V. Putting together, we have the following effective dynamical matrix for the two modes

$$\begin{bmatrix} (\Omega + \delta/2 + i\gamma)^2 & V(a + ib\Omega) + ic\Omega \\ -V(a + ib\Omega) + ic\Omega & (\Omega - \delta/2 + i\gamma)^2 \end{bmatrix}. \tag{9}$$

Here, a and b are non-zero only in the presence of voltage bias in the e-bath, which correspond to the currend-induced non-conservative and effective Lorentz force, respectively[39]. Meanwhile, c and γ account for the damping due to coupling to ph-bath and/or e-bath. If we ignore the energy dependence of electron spectral function within the voltage bias window, $a = \mathrm{Imtr}[M^1 A_L M^2 A_R]/\pi$ becomes constant, $b = 0$. This approximation is valid if the electron bandwidth D is much larger than the corresponding mode energy $\hbar\Omega$, i.e., $D \gg \hbar\Omega$. Figure 6 shows a typical example for this model. We have plotted the imaginary (a), the real (b) part of the eigen values as a function of bias. The exceptional point corresponds to the place where both parts are the same for the two modes. Additionally, at this point the inner product of the two eigen vectors takes the maximum value 1, meaning that the eigen vectors coalesce.

IV. CONCLUSIONS

In summary, we have shown that a normal two-probe electron conductor can be effectively viewed as EHP baths with chemical potential determined by the applied voltage bias. This is made possible by introducing the inter-electrode charge transfer EHPs. Properties of the EHP baths can be engineered through tuning the parameters of the conductor and the external voltage bias. This bath engineering provides an efficient way of controlling hybrid energy and thermoelectric transport in electron-boson junctions.

ACKNOWLEDGMENTS

The authors thank J.-S. Wang and M. Brandbyge for discussions. This work is supported by the National Natural Science Foundation of China (Grant No. 21873033), the National Key Research and Development Program of China (Grant No. 2017YFA0403501) and the program for HUST academic frontier youth team.

[1] Yoseph Imry and Rolf Landauer, “Conductance viewed as transmission,” Rev. Mod. Phys. **71**, S306–S312 (1999).
[2] Teemu Ojanen and Antti-Pekka Jauho, “Mesoscopic photon heat transistor,” Physical review letters **100**, 155902 (2008).
[3] S.-A. Biehs, E. Rousseau, and J.-J. Greffet, “Mesoscopic description of radiative heat transfer at the nanoscale,” Phys. Rev. Lett. **105**, 234301 (2010).
[4] Zu-Quan Zhang, Jing-Tao Lü, and Jian-Sheng Wang, “Energy transfer between two vacuum-gapped metal plates: Coulomb fluctuations and electron tunneling,” Phys. Rev. B **97**, 195450 (2018).
[5] Philippe Ben-Abdallah and Svend-Age Biehs, “Near-field thermal transistor,” Phys. Rev. Lett. **112**, 044301 (2014).
[6] Luis G. C. Rego and George Kirczenow, “Quantized thermal conductance of dielectric quantum wires,” Phys. Rev.

Lett. **81**, 232–235 (1998).

[7] N. Mingo and D. A. Broido, "Carbon nanotube ballistic thermal conductance and its limits," Phys. Rev. Lett. **95**, 096105 (2005).

[8] Takahiro Yamamoto and Kazuyuki Watanabe, "Nonequilibrium green's function approach to phonon transport in defective carbon nanotubes," Phys. Rev. Lett. **96**, 255503 (2006).

[9] Jian-Sheng Wang, Jian Wang, and Nan Zeng, "Nonequilibrium green's function approach to mesoscopic thermal transport," Physical Review B **74**, 033408 (2006).

[10] Jian-Sheng Wang, Nan Zeng, Jian Wang, and Chee Kwan Gan, "Nonequilibrium green's function method for thermal transport in junctions," Physical Review E **75**, 061128 (2007).

[11] J-S Wang, Jian Wang, and JT Lü, "Quantum thermal transport in nanostructures," The European Physical Journal B **62**, 381–404 (2008).

[12] Tomi Ruokola, Teemu Ojanen, and Antti-Pekka Jauho, "Thermal rectification in nonlinear quantum circuits," Physical Review B **79**, 144306 (2009).

[13] Nianbei Li, Jie Ren, Lei Wang, Gang Zhang, Peter Hänggi, and Baowen Li, "Colloquium: Phononics: Manipulating heat flow with electronic analogs and beyond," Reviews of Modern Physics **84**, 1045 (2012).

[14] Edward Taylor and Dvira Segal, "Quantum bounds on heat transport through nanojunctions," Physical review letters **114**, 220401 (2015).

[15] Chiao-Hsuan Wang and Jacob M Taylor, "Landauer formulation of photon transport in driven systems," Physical Review B **94**, 155437 (2016).

[16] Baigeng Wang, Jian Wang, Jin Wang, and D. Y. Xing, "Spin current carried by magnons," Phys. Rev. B **69**, 174403 (2004).

[17] Klaus Kuhnke, Christoph Große, Pablo Merino, and Klaus Kern, "Atomic-scale imaging and spectroscopy of electroluminescence at molecular interfaces," Chemical Reviews **117**, 5174–5222 (2017).

[18] Michael Galperin, "Photonics and spectroscopy in nanojunctions: a theoretical insight," Chem. Soc. Rev. **46**, 4000–4019 (2017).

[19] Natalia L. Schneider, Guillaume Schull, and Richard Berndt, "Optical probe of quantum shot-noise reduction at a single-atom contact," Phys. Rev. Lett. **105**, 026601 (2010).

[20] N. L. Schneider, J. T. Lü, M. Brandbyge, and R. Berndt, "Light emission probing quantum shot noise and charge fluctuations at a biased molecular junction," Phys. Rev. Lett. **109**, 186601 (2012).

[21] Zhifeng Huang, Fang Chen, Roberto D'agosta, Peter A Bennett, Massimiliano Di Ventra, and Nongjian Tao, "Local ionic and electron heating in single-molecule junctions," Nature nanotechnology **2**, 698 (2007).

[22] Zvi Ioffe, Tamar Shamai, Ayelet Ophir, Gilad Noy, Ilan Yutsis, Kobi Kfir, Ori Cheshnovsky, and Yoram Selzer, "Detection of heating in current-carrying molecular junctions by raman scattering," Nature nanotechnology **3**, 727 (2008).

[23] Jing-Tao Lü, Rasmus B. Christensen, Jian-Sheng Wang, Per Hedegård, and Mads Brandbyge, "Current-Induced Forces and Hot Spots in Biased Nanojunctions," Phys. Rev. Lett. **114**, 096801 (2015).

[24] R Härtle and M Thoss, "Resonant electron transport in single-molecule junctions: Vibrational excitation, rectification, negative differential resistance, and local cooling," Physical Review B **83**, 115414 (2011).

[25] R Härtle and M Thoss, "Vibrational instabilities in resonant electron transport through single-molecule junctions," Physical Review B **83**, 125419 (2011).

[26] R Härtle, C Schinabeck, M Kulkarni, D Gelbwaser-Klimovsky, M Thoss, and U Peskin, "Cooling by heating in nonequilibrium nanosystems," Physical Review B **98**, 081404 (2018).

[27] Michael Galperin, Keiji Saito, Alexander V Balatsky, and Abraham Nitzan, "Cooling mechanisms in molecular conduction junctions," Physical Review B **80**, 115427 (2009).

[28] Lena Simine and Dvira Segal, "Vibrational cooling, heating, and instability in molecular conducting junctions: full counting statistics analysis," Physical Chemistry Chemical Physics **14**, 13820–13834 (2012).

[29] Jacob Lykkebo, Giuseppe Romano, Alessio Gagliardi, Alessandro Pecchia, and Gemma C. Solomon, "Single-molecule electronics: Cooling individual vibrational modes by the tunneling current," The Journal of Chemical Physics **144**, 114310 (2016), https://doi.org/10.1063/1.4943578.

[30] Linxiao Zhu, Anthony Fiorino, Dakotah Thompson, Rohith Mittapally, Edgar Meyhofer, and Pramod Reddy, "Near-field photonic cooling through control of the chemical potential of photons," Nature **566**, 239 (2019).

[31] Martin Head-Gordon and John C. Tully, "Molecular dynamics with electronic frictions," The Journal of Chemical Physics **103**, 10137–10145 (1995).

[32] Wenjie Dou and Joseph E. Subotnik, "Perspective: How to understand electronic friction," The Journal of Chemical Physics **148**, 230901 (2018), https://doi.org/10.1063/1.5035412.

[33] Jing-Tao Lü, Mads Brandbyge, Per Hedegård, Tchavdar N. Todorov, and Daniel Dundas, "Current-induced atomic dynamics, instabilities, and Raman signals: Quasiclassical Langevin equation approach," Phys. Rev. B **85**, 245444 (2012).

[34] Jing-Tao Lü, Jian-Sheng Wang, Per Hedegård, and Mads Brandbyge, "Electron and phonon drag in thermoelectric transport through coherent molecular conductors," Physical Review B **93**, 205404 (2016).

[35] Lifa Zhang, Jing-Tao Lü, Jian-Sheng Wang, and Baowen Li, "Thermal transport across metal–insulator interface via electron–phonon interaction," Journal of Physics: Condensed Matter **25**, 445801 (2013).

[36] Jie Ren and Jian-Xin Zhu, "Heat diode effect and negative differential thermal conductance across nanoscale metal-dielectric interfaces," Physical Review B **87**, 241412 (2013).

[37] O. Entin-Wohlman, Y. Imry, and A. Aharony, "Three-terminal thermoelectric transport through a molecular junction," Phys. Rev. B **82**, 115314 (2010).

[38] Rafael Sánchez and Markus Büttiker, "Optimal energy quanta to current conversion," Phys. Rev. B **83**, 085428 (2011).

[39] Jing-Tao Lü, Mads Brandbyge, and Per Hedegård, "Blowing the Fuse: Berry's Phase and Runaway Vibrations in Molecular Conductors," Nano Lett. **10**, 1657–1663 (2010).